Applied Surface Science 485 (2019) 35–40

Contents lists available at ScienceDirect

Applied Surface Science

journal homepage: www.elsevier.com/locate/apsusc

Full length article

Surface modification of Sb_2O_3 nanoparticles with dioctylphthalate

Jianlin Xu*, Chengcheng Xu, Lei Niu, Chenghu Kang

State Key Laboratory of Advanced Processing and Recycling of Non-ferrous Metals, Lanzhou University of Technology, Lanzhou 730050, China
Baiyin Research Institute of Novel Materials, Lanzhou University of Technology, Baiyin 730900, China

ARTICLE INFO

Keywords:
Dioctylphthalate
Sb_2O_3 nanoparticles
Surface modification
Mechanochemical method

ABSTRACT

Dioctylphthalate (DOP) was used as the surface modifier to modify the surface of Sb_2O_3 nanoparticles by mechanical ball milling in this paper. The surface properties of Sb_2O_3 nanoparticles were characterized by XRD, Fourier transform infrared spectroscopy (FT-IR), surface contact angle measuring instrument, Zeta potentiometer and transmission electron microscope (TEM). The surface structure of Sb_2O_3 nanoparticles and the adsorption mode of DOP were studied, and the effects of different mass fraction of DOP on the dispersion and stability of Sb_2O_3 nanoparticles were analyzed. The results show that DOP can successfully coat on the surface of Sb_2O_3 nanoparticle by using mechanochemical method and significantly improve the dispersion of the modified Sb_2O_3 nanoparticles. With increasing of the mass fraction of DOP, the dispersion of Sb_2O_3 nanoparticles was gradually improved. When the mass fraction of DOP was 7 wt%, the average particle size of Sb_2O_3 nanoparticles was the smallest, and was 48 nm. However, with the increase of the mass fraction of DOP, the absolute Zeta potential of Sb_2O_3 nanoparticles gradually decreased and then tended to be stable finally.

1. Introduction

Antimony trioxide (Sb_2O_3), as an important inorganic flame-retardant synergist, is widely used in polymer materials such as plastics, textiles, rubber and coatings [1–3]. Especially in polymer composites with halogen-antimony collaborative system, Sb_2O_3 can decrease the mass fraction of the halogen flame retardants and reduce combustion smoke amount of the composites. Meanwhile, the flame retardancy of composites can be improved significantly. Some studies have shown that the particle size of Sb_2O_3 has an obvious effect on the flame retardancy of polymer composites. When the particle size of Sb_2O_3 is reduced from the micron level to nanometer level, the flame retardancy of the matrix material is improved significantly under the same conditions [4,5]. However, the flame retardancy of nanocomposites is not only affected by the particle size and synergistic effect with other flame retardants, but also depend on whether the inorganic nanoparticles can be uniformly dispersed in organic matrix materials. It is well known that nanoparticles agglomerate easily due to their high surface energy, resulting in decreasing of the dispersion degree of nanoparticles in organic matrix. The poor dispersion of nanoparticles makes the stability of the composite system worse, and ultimately affects the product performance of the composites. Therefore, it is particularly important to enhance the dispersion and stability of nanoparticle in organic matrix. According to DVLO theory [6], the properties of dispersed media and the interactions between particles in the media can determine the stability of colloidal system, including van der Waals' force (V_A) and electric double-layer repulsive force (V_R). Therefore, researchers try to improve the dispersion and stability of nanoparticles in the medium by various methods. For example, under the action of mechanical force, some reagents such as polyelectrolyte or surfactant can adhere to the surface of nanoparticles, improve the electrostatic interaction or space steric effect between particles and facilitate the dispersion of nanoparticles [7–9]. Nanoparticles can also be modified by various surface modifiers. The surface modification of nanoparticles can reduce the surface energy and improve the dispersibility of inorganic nanoparticles in organic matrix [10].

Dioctylphthalate (DOP) is one of the main plasticizers for polymer products. However, DOP migrates from polymer product easily, resulting in serious pollution of the surrounding medium and the deterioration of mechanical properties [11]. Due to high surface energy and a large number of unsaturated bonds of atoms, nanoparticles can easily bond with polar plasticizer DOP, which has been applied in some fields. Some studies show that the polar bonds of DOP can be attracted by inorganic nanoparticles, so the anti-migration properties of DOP can be strengthened. For example, Yan Wen Zhou et al. [12] studies the effects of nano-particles (nano-$CaCO_3$, nano-SiO_2 and MMT modified by

* Corresponding author at: State Key Laboratory of Advanced Processing and Recycling of Non-ferrous Metals, Lanzhou University of Technology, Lanzhou 730050, China.
E-mail address: xujl@lut.cn (J. Xu).

https://doi.org/10.1016/j.apsusc.2019.04.007
Received 30 December 2018; Received in revised form 24 March 2019; Accepted 1 April 2019
Available online 22 April 2019
0169-4332/

organic modifier) on DOP migration and tensile properties of flexible PVC sheets and found that the polar bonds of DOP can be attracted by inorganic nanoparticles, so the anti-migration properties of PVC can be strengthened. As a result, in flexible PVC products with DOP as plasticizer, using DOP as surface modifier of inorganic filler can not only improve the compatibility between inorganic filler and organic matrix, but also improve the anti-migration properties of PVC. In this work, the surface of Sb_2O_3 nanoparticles was modified by mechanical ball grinding method using DOP as surface modifier. Surface structure of Sb_2O_3 nanoparticles were studied by XRD, transmission electron microscope (TEM) and infrared spectroscopy (FT-IR). And then the dispersion degree and stability properties of nanoparticles modified with different mass fraction of DOP were analyzed basing on the surface contact angle and Zeta potential.

2. Experimental

2.1. Materials

Sb_2O_3 nanoparticles were made by our laboratory and the range of particle size is 50–100 nm [13]. DOP was purchased from Laiyang Shuangshuang Chemical Co., Ltd. (Shandong, China) and its average molecular weight is 391.

2.2. Surface modification of Sb_2O_3 nanoparticles

Sb_2O_3 nanoparticles were modified by OM-3SP04 planetary ball mill (Nanjing Laibu Science and Technology Industry Co., Ltd., China). In this process, 5 g Sb_2O_3 nanoparticles, 20 ml ethyl alcohol and different mass fraction DOP will be mixed in ball milling jar and the mass ratio of balls to powders was 24:1. The rotational speed was 400 rpm/min and the milling time was 6 h. The resulting samples and their modification conditions were listed in Table 1. After ball milling, the samples were washed with ethyl alcohol, and then filtered and dried for 12 h in vacuum drying oven.

2.3. Characterization of Sb_2O_3 nanoparticles

The phases of the sample were analyzed by XRD (Ultima IV, Japan Science Corporation), where the 2θ range is from 5° to 80° and the scanning speed is 2°/min, using Cu-Kα radiation (λ = 0.154 nm) at room temperature.

Fourier transform infrared spectrometer (FT-IR, NEXUS-670, American Thermal Power Company) was used to characterize the surface adsorption of Sb_2O_3 nanoparticles. Before measurement, 1 mg particles sample was mixed with 200 mg KBr and then prepared by pressing into slices. The spectral range was 4000–400 cm^{-1}, the scanning speed was 4 cm^{-1} and the scanning frequency was 32 times.

The morphology and dispersion of Sb_2O_3 nanoparticles were observed by transmission electron microscopy (TEM). Firstly, the nanoparticles were dispersed into ethyl alcohol by sonication to form particle suspension. Then, the mesh was immersed in the suspension for a while and then taken out to dry in air. Finally, the mesh was put into the TEM (JEM-210, Japanese Electronics Company) to characterize the morphology and dispersion of modified and unmodified Sb_2O_3 nanoparticles. The software of Nano measurer 1.2 was used to calculate Sb_2O_3 nanoparticles sizes basing on TEM images.

Table 1
Mass ratio of DOP and Sb_2O_3 nanoparticles.

Number	Sample	DOP/wt%	Sb_2O_3/wt%
1#	P-Sb_2O_3	0	100
2#	1% DOP-Sb_2O_3	1	99
3#	3% DOP-Sb_2O_3	3	97
4#	5% DOP-Sb_2O_3	5	95
5#	7%DOP-Sb_2O_3	7	93
6#	10%DOP-Sb_2O_3	10	90

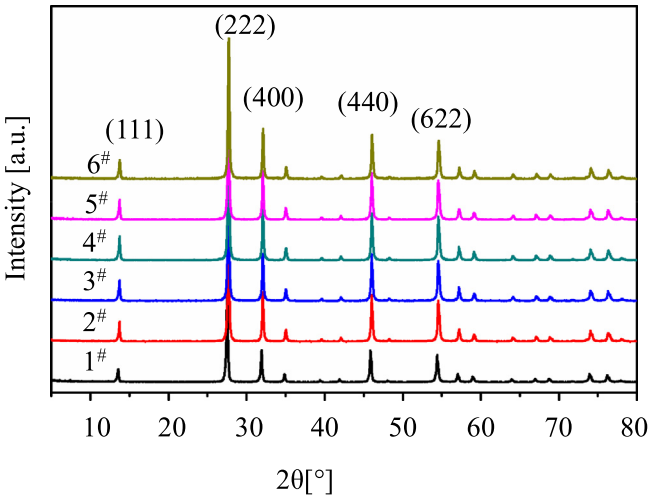

Fig. 1. XRD pattern of experimental Sb_2O_3 nanoparticles.

A set of glass plate was treated by Sb_2O_3 nanoparticles and then the contact angles formed by water against the glass plate surface were measured by JGW-360A optical contact angle measuring instrument (Xiamen Chongda Intelligent Technology Co., Ltd).

Zeta potential was determined by using a JS94H Micro electrophoresis (Shanghai Zhongchen Digital Technology Equipment Co., Ltd.). The pH value of the Sb_2O_3 nanoparticles suspension, which was prepared as describe above, was adjusted as 7 when the Zeta potential was measured.

3. Results and discussion

3.1. XRD of Sb_2O_3 nanoparticles

Fig. 1 shows the XRD spectra curve of Sb_2O_3 nanoparticles modified with different mass fraction of DOP. It can be seen that there are some very sharp diffraction peaks from 5° to 80° of 2θ corresponding to nature phases of Sb_2O_3. Comparing with diffraction spectra of experimental samples, it can be found that crystal structure of Sb_2O_3 nanoparticles modified with DOP doesn't change.

3.2. FT-IR of Sb_2O_3 nanoparticles

Fig. 2 shows the FT-IR spectra curves of Sb_2O_3 nanoparticles experimental samples. For sample 1#, it can be seen that the peaks at 3430 cm^{-1} and 1631 cm^{-1} can be respectively attributed to the stretching vibration and bending vibration of hydroxyl bond (–OH) [14]. Comparing these infrared spectra of samples 1#, 3# and 5#, it is found that the hydroxy stretching vibration peak and bending vibration peak of sample 3# are weaken significantly, and the hydroxy stretching vibration peak and bending vibration peak of sample 5# almost disappears. At the same time, a new carbonyl absorption peak appears near 1728 cm^{-1}, and the new peak falls within the theoretical value range of 1730 cm^{-1}–1700 cm^{-1}, which indicates the formation of hydrogen bonds between the carbonyl and the Sb_2O_3 nanoparticles. Therefore, it can be explained that DOP and the hydroxyl group on the surface of Sb_2O_3 nanoparticles take place hydrogen bond adsorption. In addition, there are three new characteristic absorption peaks in the infrared spectra of samples 3# and 5#. The peak at 2918 cm^{-1} is assigned asymmetric stretching vibration peak of alkyl group. The peak at 1443 cm^{-1} is associated with skeleton vibrational peak of benzene ring and the peak at 1285 cm^{-1} is belonged to ether bond absorption peak. The disappearance of characteristic absorption peaks and appearance of

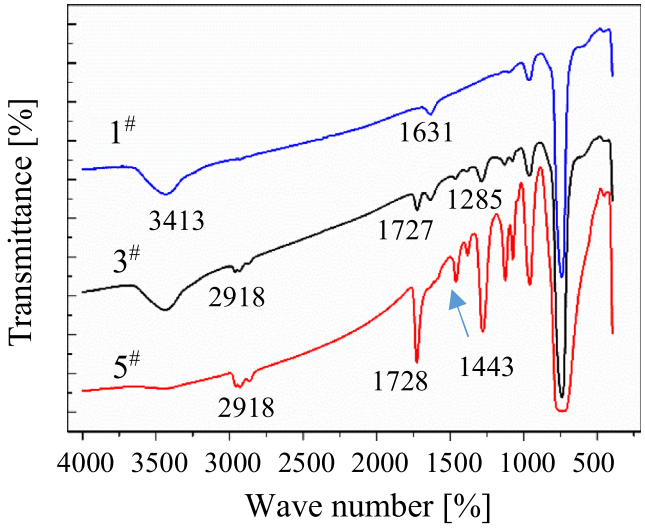

Fig. 2. FT-IR spectra of experimental Sb_2O_3 nanoparticles.

new peaks indicate that DOP is successfully attached on the surface of Sb_2O_3 nanoparticles. Comparing the infrared spectra of samples $3^{\#}$ and $5^{\#}$, these new absorption peaks of sample $5^{\#}$ are stronger than that of sample $3^{\#}$. It indicates that the hydroxyl groups on the surface of modified Sb_2O_3 nanoparticles are gradually replaced by DOP. And the higher the mass fraction of DOP, the more completely hydroxyl groups on the surface of Sb_2O_3 nanoparticles are replaced.

3.3. Surface contact angle of Sb_2O_3 nanoparticles

Fig. 3 shows the surface contact angle of unmodified and modified Sb_2O_3 nanoparticles. Dispersion of inorganic particles fillers in organic matrix is related to the particles surface wettability and good surface wettability can promote inorganic fillers and organic matrix form uniform dispersion system. The surface wettability of nanoparticles can be estimated indirectly by measuring surface contact angle [15]. A smaller contact angle formed on the sample surface reflects to a better wettability of the liquids with sample.

As can be seen from Fig. 3, the surface contact angle of sample $1^{\#}$ is 11.8°, the contact angle of sample $2^{\#}$ is 65.5°, the contact angle of sample $3^{\#}$ is 70.1°, the contact angle of sample $4^{\#}$ is 82.7°, the contact angle of sample $5^{\#}$ is 93.3° and the contact angle of sample $6^{\#}$ is 90.7°. In general, the hydrophobic surface has a lower wettability. A contact angle with 0° means complete wetting and a contact angle with 180° means complete nonwetting. The particle surface has wettability when its contact angle is less than 90°. And the particle surface has unwettability when its contact angle is more than 90° [16]. The higher the contact angle, the lower the surface energy [17]. Therefore, decreasing the contact angle can enlarge the hydrophilicity of the particle surface. From the above results, the surface of Sb_2O_3 nanoparticles modified by DOP has obvious hydrophobic surface which surface energy of inorganic particle decrease. It can be found that the contact angle of nanoparticles increases with increasing of the mass fraction of DOP, which modified the surface of Sb_2O_3 nanoparticles. DOP is hydrophobicity because it contains ester group. Therefore, when the mass fraction of DOP increases, the hydroxyl group adsorbed on the surface of Sb_2O_3 nanoparticles is replaced completely, and the amount of DOP covered on the surface of Sb_2O_3 nanoparticles is increased. However, it can be seen from samples $5^{\#}$ and $6^{\#}$ that when the mass fraction of DOP exceeds a certain value, the influence of the mass fraction of DOP on Sb_2O_3 nanoparticles decreases. This is because the DOP absorbed on the Sb_2O_3 nanoparticles is limited. Therefore, when the mass fraction of DOP is lower than 7 wt%, with the increasing of mass fraction of DOP, the larger the contact angle measured by Sb_2O_3 nanoparticles is. Namely, the lower the surface energy of the particles, the better the wettability of Sb_2O_3 nanoparticles. When it exceeds 7 wt%, the contact angle of Sb_2O_3 nanoparticles doesn't change obviously.

3.4. Zeta potential of Sb_2O_3 nanoparticles

Fig. 4 shows the relationship curve between Zeta potential of Sb_2O_3 nanoparticles and the mass fraction of DOP. Zeta potential is a physical property which is showed by particles in suspension. It can be used to optimize the formulations of emulsion and suspension. There are many origins of surface charge depending on the nature of particles and its surrounding medium. The absolute potential reflects the potential stability of the colloidal system. If all the particles in the suspensions show a large positive or negative potential, there is a repulsion interaction between the particles, and the tendency of agglomeration between the particles will be reduced because of the repulsive effect. Some studies show that the surface charge polarity of nanoparticles is closely related to the acidity and alkalinity of suspension [18]. The Sb_2O_3 nanoparticles are in the equipotential state when the pH value is about 4.

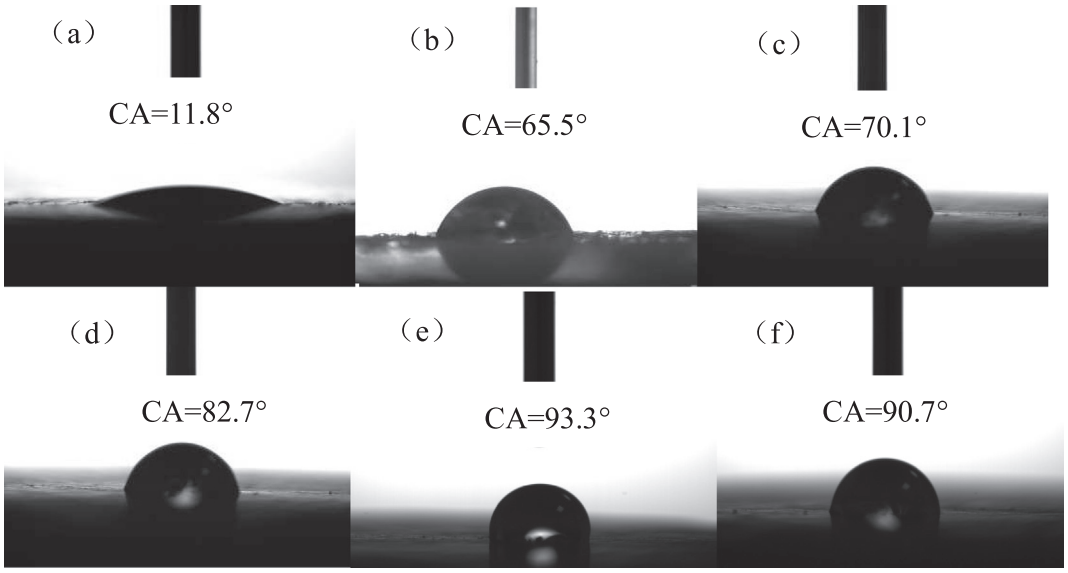

Fig. 3. Contact angle of Sb_2O_3 nanoparticles (a) $1^{\#}$; (b) $2^{\#}$; (c) $3^{\#}$; (d) $4^{\#}$; (e) $5^{\#}$; (f) $6^{\#}$.

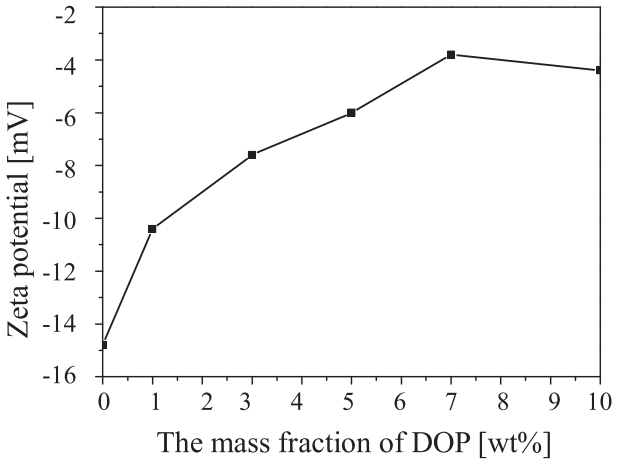

Fig. 4. Zeta potential of Sb_2O_3 nanoparticles.

When the pH value of suspension is more than 4, the adsorbed hydroxyl group on the surface of Sb_2O_3 nanoparticles loses H^+, and Sb_2O_3 nanoparticles show electronegativity. When the pH value of suspension is less than 4, the adsorbed hydroxyl group on the surface of Sb_2O_3 nanoparticles obtains H^+, Sb_2O_3 nanoparticles show electropositive.

It can be seen from Fig. 4 that Zeta absolute potential value of Sb_2O_3 nanoparticles gradually decreases with increasing of the mass fraction of DOP. This is because as the mass fraction of DOP increases, the adsorbed hydroxyl group on the surface of Sb_2O_3 nanoparticles is gradually replaced by DOP, which makes DOP cover the surface of Sb_2O_3 nanoparticles, thus making the negative charge on the surface of Sb_2O_3 nanoparticles offset. Therefore, the decreasing of Zeta absolute potential value indicates that DOP is successfully adsorbed on the surface of Sb_2O_3 nanoparticles. However, when the mass fraction of DOP is 10 wt %, Zeta potential absolute value of the Sb_2O_3 nanoparticles has little change compared with that of 7 wt%. This is because the specific surface area of nanoparticles is constant, so the DOP that can be coated is also constant. Therefore, when the DOP exceeds a certain amount, the particle potential value tends to be stable.

3.5. Morphology and particle size distribution of Sb_2O_3 nanoparticles

Fig. 5 shows some TEM images and particle size distribution map of experimental Sb_2O_3 nanoparticles. It can be seen from sample $1^{\#}$ that the unmodified Sb_2O_3 nanoparticles have irregular shape and their particle size is not uniform, and there are some aggregates indicating taking place aggregation of unmodified Sb_2O_3 nanoparticles. Because the surface of unmodified Sb_2O_3 nanoparticles has a lot of adsorption hydroxyl groups in different states, these nanoparticles can be aggregated by weak hydrogen bond polymerization. The average particle size of sample $1^{\#}$ is 56 nm. It can be found from the samples of $2^{\#}$, $3^{\#}$, $4^{\#}$ and $5^{\#}$ that the dispersion of modified Sb_2O_3 nanoparticles is significantly improved, the agglomeration phenomenon is significantly reduced, and the modified Sb_2O_3 nanoparticles are covered with thin films. Comparing the samples of $2^{\#}$, $3^{\#}$, $4^{\#}$ and $5^{\#}$, it can be seen that the dispersion degree of Sb_2O_3 nanoparticles gradually improves with increasing of the mass fraction of DOP. Their average particle sizes are respectively 53 nm, 52 nm, 50 nm and 48 nm. There are two reasons for good dispersion states of modified Sb_2O_3 nanoparticles. One is mechanical ball milling effect. It can activate the surface of the nanoparticles to produce free radicals or ions which can promote the chemical adsorption between the modifier and the surface of nanoparticles [7,19]. Meanwhile, mechanical ball milling effect can break up agglomerates to be secondarily dispersed. In the process of modification, the mechanical force continuously provides new surface and energy for the nanoparticles and the modifier, resulting in full physical and

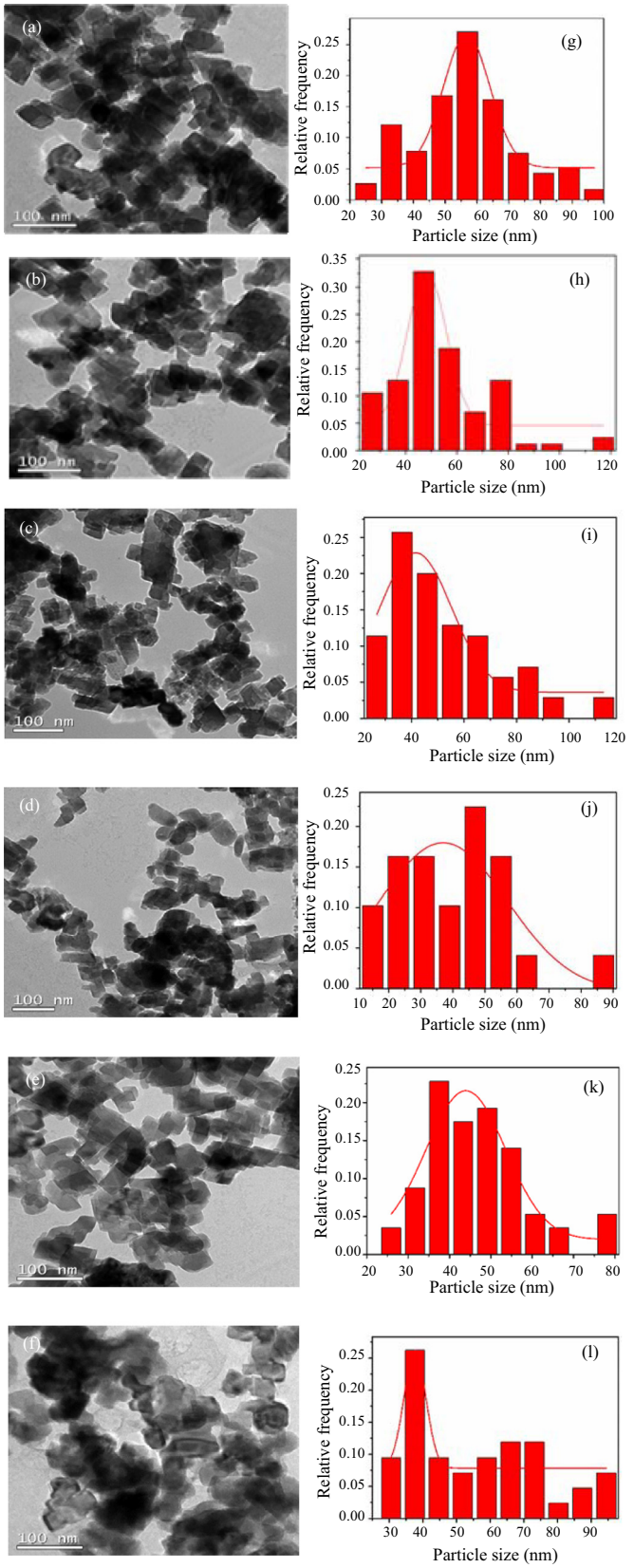

Fig. 5. TEM images of Sb_2O_3 nanoparticles (a) $1^{\#}$; (b) $2^{\#}$; (c) $3^{\#}$; (d) $4^{\#}$; (e) $5^{\#}$; (f) $6^{\#}$ and particle size distribution of Sb_2O_3 nanoparticles (g) $1^{\#}$; (h) $2^{\#}$; (i) $3^{\#}$; (j) $4^{\#}$; (k) $5^{\#}$; (l) $6^{\#}$.

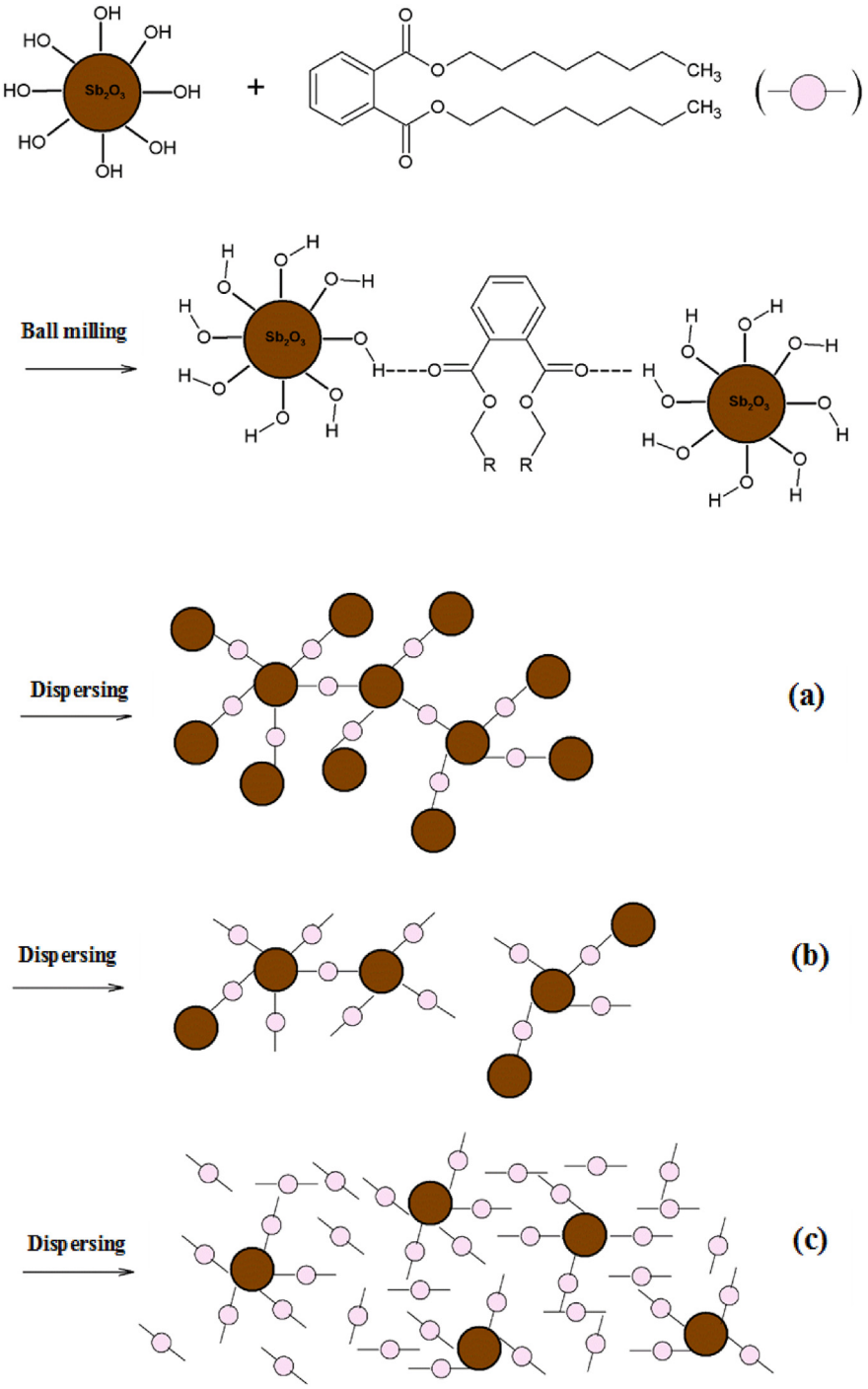

Fig. 6. General schematic of the modification of Sb_2O_3 nanoparticles.

chemical reaction between the nanoparticle and the modifier [20,21]. Another reason is that DOP modifies Sb_2O_3 nanoparticles to form a coating which can weaken or shield the agglomeration of nanoparticles. Because of the space steric effect of the coating, it is difficult for modified Sb_2O_3 nanoparticles to agglomerate again. However, a small amount of DOP can't completely replace hydroxyl groups on the surface of the Sb_2O_3 nanoparticles and form a complete coating layer on the surface of the nanoparticles. Therefore, the higher the mass fraction of DOP, the better the dispersion effect of the modified Sb_2O_3 nanoparticles will be. In addition, it can be found by comparing $5^{\#}$ and $6^{\#}$ that Sb_2O_3 nanoparticles are flocculent particles, which indicates the agglomeration phenomenon takes place between the nanoparticles, when the mass fraction of DOP is 10 wt%. The reason is that the excess DOP molecules can cause flocculation of nanoparticles by means of bridging action of saturation coating with the increasing of the mass fraction of DOP.

3.6. Modification mechanism of Sb_2O_3 nanoparticles

Fig.6 shows the general schematic of the modification of Sb_2O_3 nanoparticles. Combined with FT-IR, it can be found that there are a large number of adsorbed hydroxyl groups on the surface of Sb_2O_3 nanoparticles. Because the oxygen atoms of ester group in DOP have lone pair electrons and the hydrogen atoms in hydroxyl group have

vacant orbits, the two structures can provide conditions for the formation of hydrogen bonds. There are three situations when DOP modify Sb_2O_3 nanoparticles. The first one is that when the mass fraction of DOP is low, each DOP molecule can absorb Sb_2O_3 nanoparticles to the maximum extent, as shown in Fig. 6(a). At this time, the surface of Sb_2O_3 nanoparticles is not completely coated by DOP. The second is that the single molecule of DOP is adsorbed by the active atom of the surface of the Sb_2O_3 nanoparticles to form a complete coating layer with increasing of the mass fraction of DOP. At this time, the molecule of DOP plays a role of steric hindrance, as shown in Fig. 6(b). The last one is that when the mass fraction of DOP increases to saturation, the excess DOP molecules will cause flocculation of Sb_2O_3 nanoparticles through bridging action, as shown in Fig. 6(c). This is consistent with the results of Zeta potential, surface contact angle and TEM characterization.

4. Conclusions

In this work, the Sb_2O_3 nanoparticles modified by different mass fraction of Dioctylphthalate (DOP) were characterized and the following conclusions were drawn from the study:

(1). DOP can be successfully adsorbed to the surface of Sb_2O_3 nanoparticles by means of surface modification. The higher the mass fraction of DOP is, the more complete the hydroxyl substitution connection is, and the more complete the coating layer is on the surface of Sb_2O_3 nanoparticles.
(2). Compared with the unmodified Sb_2O_3 nanoparticles, the wettability of modified Sb_2O_3 nanoparticles was significantly improved. The higher the mass fraction of DOP, the greater the contact angle of Sb_2O_3 nanoparticles. As a result, particles have the lower surface energy and the better wettability. However, the influence of DOP on surface contact angle became very humble when the mass fraction of DOP exceed 7 wt%.
(3). The absolute value of Zeta potential of modified Sb_2O_3 nanoparticles is smaller than that of unmodified Sb_2O_3 nanoparticles. The more DOP is used, the smaller the absolute potential value is, and it tends to be stable.
(4). The dispersion of modified Sb_2O_3 nanoparticles was significantly affected. With the increasing of the mass fraction of DOP, Sb_2O_3 nanoparticles appeared agglomeration–dispersion–reagglomeration state.

Acknowledgment

The work was supported by the National Nature Science Foundation of China (No. 51761025) and the Science and Technology Project Funds of Gansu Province (No. 17CC2JD075).

References

[1] E. Gallo, B. Schartel, D. Acierno, P. Russo, Flame retardant biocomposites: synergism between phosphinate and nanometric metal oxides, Eur. Polym. J. 47 (2011) 1390–1401, https://doi.org/10.1016/j.eurpolymj.2011.04.001.
[2] G. Guido, K. Daiki, K. Tomohito, B. Thallada, Y. Toshiaki, Effect of heating rate on the pyrolysis of high-impact polystyrene containing brominated flame retardants: fate of brominated flame retardants, J. Mater. Cycles Waste Manage. 14 (2012) 259–265, https://doi.org/10.1007/s10163-012-0067-8.
[3] K.M. Xu, K.F. Li, Y.P. Deng, X. Yan, X.C. Ping, Effect of inorganic flame retardant on the properties of wood/PVC composites, Adv. Mater. Res. 430–432 (2012) 110–114, https://doi.org/10.4028/www.scientific.net/AMR.430-432.110.
[4] Z. Mirdamadian, D. Ghanbari, Synergistic effect between Sb_2O_3 nanoparticles–trichloromelamine and carbon nanotube on the flame retardancy and thermal stability of the cellulose acetate, J. Clust. Sci. 25 (2014) 925–936, https://doi.org/10.1007/s10876-013-0673-1.
[5] M.M. Si, J. Feng, J.W. Hao, L.S. Xu, J.X. Du, Synergistic flame retardant effects and mechanisms of nano-Sb_2O_3 in combination with aluminum phosphinate in poly (ethylene terephthalate), Polym. Degrad. Stab. 100 (2014) 70–78, https://doi.org/10.1016/j.polymdegradstab.2013.12.023.
[6] J.E. Verwey, Theory of the stability of lyophobic colloids, J. Phys. Colloid Chem. 10 (1955) 224–225, https://doi.org/10.1016/0095-8522(55)90030-1.
[7] H. Ding, S.C. Lu, G.X. Du, Surface modification of wollastonite by the mechano-activated method and its properties, Int. J. Miner. Metall. Mater. 18 (2011) 83–88, doi:10.1007/s12613-011-0404-2.
[8] M. Kimata, M. Hasegawa, N. Kotake, Mechanochemical polymerization of methyl methacrylate initiated by the grinding of quartz in an n-heptane solvent, Powder Technol. 235 (2013) 336–340, https://doi.org/10.1016/j.powtec.2012.10.027.
[9] J. Lin, H. Chen, Y. Yuan, Y. Ji, Mechanochemically conjugated PMHS/nano-SiO_2 hybrid and subsequent optimum grafting density study, Appl. Surf. Sci. 257 (2011) 9024–9032, https://doi.org/10.1016/j.apsusc.2011.05.093.
[10] J.L. Xu, S.G. Zhou, L. Niu, W.L. Yang, C.C. Wang, C. Wen, Effect of Sb_2O_3 modified by various surface active agents on flame retardant properties of PVC composite, Mater. Eng. 44 (2016) 64–69, https://doi.org/10.11868/j.issn.1001-4381.2016.08.011.
[11] J.F.J. Coelho, M. Carreira, Gonçalves, M.O.F Pedro, A.V. Popov, M.H. Gil, Processability and characterization of poly (vinyl chloride)-b-poly (n-butyl acrylate)-b-poly (vinyl chloride) prepared by living radical polymerization of vinyl chloride. Comparison with a flexible commercial resin formulation prepared with PVC and dioctyl phthalate, J. Vinyl Addit. Technol. 12 (2010) 156–165, doi:https://doi.org/10.1002/vnl.20088.
[12] Y.W. Zhou, Y. Xiao, X.H. Li, B. Wang, Effects of nano-particles on DOP migration and tensile properties of flexible PVC sheets, Adv. Mater. Res. 548 (2012) 119–122, https://doi.org/10.4028/www.scientific.net/AMR.548.119.
[13] J.L. Xu, L. Zhang, S.G. Zhou, C. Feng, Effect of surface active agents on nanometer Sb_2O_3 power prepared by ball milling, Rare Metal Mater. Eng. 12 (2014) 3003–3307 http://xueshu.baidu.com/usercenter/paper/show?paperid=17a1f554e7c81ab82b3fb2b393d6bb0f&site=xueshu_se&hitarticle=1>.
[14] C.M. Koretsky, D.A. Sverjensky, J.W. Salisbury, D.M. D'Aria, Detection of surface hydroxyl species on quartz, γ-alumina, and feldspars using diffuse reflectance infrared spectroscopy, Geochim. Cosmochim. Acta 61 (1997) 2193–2210, https://doi.org/10.1016/S0016-7037(97)00056-2.
[15] T. Nihei, S. Kurata, Y. Kondo, K. Umemoto, N. Yoshino, T. Teranaka, Enhanced hydrolytic stability of dental composites by use of fluoroalkyltrimethoxysilanes, J. Dent. Res. 81 (2002) 482–486, https://doi.org/10.1177/154405910208100710.
[16] X.K. Ma, N.H. Lee, H.J. Oh, J.W. Kim, C.K. Rhee, K.S. Park, Surface modification and characterization of highly dispersed silica nanoparticles by a cationic surfactant, Colloids Surf. A Physicochem. Eng. Asp. 358 (2010) 172–176, https://doi.org/10.1016/j.colsurfa.2010.01.051.
[17] Z. Heng, H. Chen, Fabrication and characterizations of a polymer hybrid OA/MA/St-TiO_2, Appl. Surf. Sci. 256 (2010) 1992–1995, https://doi.org/10.1016/j.apsusc.2009.09.033.
[18] W. Cao, Z. Li, J. Gong, G. Sheng, X. Jiang, Influence of nano-particle concentration and surface treatment on space charge behavior in nano-MgO/PP, High Voltage Eng. 41 (2015) 1495–1504 https://doi.org/10.13336/j.1003-6520.hve.2015.05.011.
[19] S.A. Barseghyan, Y. Sakka, Mechanochemical activation of aluminum powder and synthesis of alumina based ceramic composites, Ceram. Int. 39 (2013) 8141–8146, https://doi.org/10.1016/j.ceramint.2013.03.087.
[20] A. Nasser, U. Mingelgrin, Mechanochemistry: a review of surface reactions and environmental applications, Appl. Clay Sci. 67–68 (2012) 141–150, https://doi.org/10.1016/j.clay.2011.11.018.
[21] H. Ding, S.C. Lu, Y.X. Deng, G.X. Du, Mechano-activated surface modification of calcium carbonate in wet stirred mill and its properties, Trans. Nonferrous Metals Soc. China 17 (2007) 1100–1104, https://doi.org/10.1016/s1003-6326(07)60232-5.